Proceedings of the International Society Of Flexible Formwork (ISOFF) Symposium 2015, Amsterdam
16 - 17 August 2015, Amsterdam, The Netherlands

ISOFF AMSTERDAM 2015

Design process of prestressed membrane formworks for thin-shell structures

Diederik VEENENDAAL*, Philippe BLOCK[a]

*ETH Zurich, Institute of Technology in Architecture, Block Research Group
Stefano-Franscini-Platz 5, HIL H 46.2, 8093 Zurich, Switzerland
veenendaal@arch.ethz.ch

[a] ETH Zurich, Institute of Technology in Architecture, Block Research Group

Abstract

This paper describes the digital design process of a fabric formwork applied to one of several adjacent concrete shell roofs for a private arts building to be constructed in 2017 in Brooklyn, NY, USA. This work is part of a larger feasibility study that compares this construction method to existing alternatives.

Although the force distribution under load of the fresh concrete can be exactly computed for a fabric formwork, built examples show only modest spans and, where known, high construction tolerances. Among several causes, the main reason is thought to be the difficulty in reproducing the exact force distribution on site, which is more easily achieved in a discrete cable net than a continuous membrane formwork. In the latter case, the stress distribution is governed by the cutting patterns, making their design crucial to control of these tolerances. Towards this end, the design process laid out in this paper adapts the procedure for cable-net and fabric formworks to one for purely fabric formworks by computing stress distributions and flat cutting patterns.

Keywords: fabric formwork, membrane structure, optimization, concrete shell, cutting patterns

1. Introduction

Doubly curved, thin-shell concrete structures are structurally efficient systems for medium-scale spans. Typical construction methods involve complicated, custom timber or CNC-milled foam formworks. An alternative concept is to use a flexible formwork, which allows the substantial reduction of the amount of shuttering and falsework. The use of fabric formworks means that cutting patterns need to be established, which need to be compensated for stresses due to the applied concrete loads. To this end, a best-fit optimization (Van Mele & Block [16]) and design process (Veenendaal & Block [18]) intended for loaded, discrete cable nets, is adapted for application to loaded membrane structures. The scope of this paper is limited to anticlastic shells and prestressed membrane formworks, and does not address synclastic shells and air-inflated membrane formworks.

Sections 1.1 and 1.2 explain the subject and context of the present research. Section 2 presents the problem statement and objective. Section 3 describes the computational design and optimization setup, outlining a procedure to determine cutting patterns and membrane prestresses. Future work and conclusions are discussed in Sections 4 and 5.

1.1. Fabric formworks for shells

The use of fabrics as formwork for anticlastic concrete shell structures has existed in various forms since the turn of the 20th century (Veenendaal *et al.* [17]) and has been used for construction of shells (Veenendaal & Block [18]). In particular, James Waller was responsible for hundreds of fabric formed shells in the mid 20th century (Waller & Aston, [20]), and the work by Kersavage [4], Knott & Nez [5] during the 1970s has led to many dozens of hypar-like fabric formed roofs, most recently by the company TSC Global.

In the past decade, academic interest in anticlastic fabric formed shells has been strong with prototypes being constructed by the Universities of Manitoba, Canada (West & Araya [21]), Eindhoven, Netherlands (Pronk *et al.* [11]), Edinburgh, UK (Pedreschi & Lee [10]) and Brussels, Belgium (Cauberg et al. [2]). Similarly, the authors themselves have constructed cable-net and fabric formed prototypes at ETH Zurich, Switzerland (Veenendaal & Block [18], Veenendaal *et al.* [17]). Van Mele & Block [16] have additionally applied their work in support of the construction of several larger prototypes with Escobedo Construction in Texas, USA.

1.2. Private Arts Building

The design process presented in this paper, is part of a larger feasibility study to compare the use of fabric formworks to other existing alternatives, as possible construction method for the roofs of a private arts building (PAB). PAB is planned as a 1320 m^2 multi-storey building in Brooklyn, New York, USA, to be completed in 2017. The building features a cluster of four shells as part of the overall roof structure. The contours of the building are informed by structural considerations, the architectural program, daylight entry and circulation. The four doubly curved, concrete shell roofs have a total surface area of 406 m^2 (263 m^2 in plan) with spans of 7-8 m. PAB is designed by the architectural office Solid Objectives–Idenburg Liu (SO-IL) with structural engineering of the roofs carried out by Schlaich Bergermann und Partner (SBP), and additional support provided by envelope consultants Certain Measures and concrete consultants Reginald Hough Associates. The present paper is part of the consultancy offered by the Block Research Group (BRG), ETH Zurich, on the possible use of flexible formworks.

Figure 1: Visualizations of private arts building (images courtesy of SO-IL)

2. Problem statement and objectives

Fabric formworks allow extremely lightweight shuttering with little to no scaffolding directly underneath, and related savings in transportation and storage. However, built examples show only modest spans (see Section 1.1), and where known, report construction tolerances in the order of 1/100th of the span or more (Cauberg et al. [2]). By exactly computing the force distribution in a flexible formwork under load of the fresh concrete (Van Mele & Block [16]), and subsequently the unloaded, prestressed state for given material properties, it has been shown that tolerances can be

reduced to 1/1000th of the span for cable-net formworks (Veenendaal & Block [18]). To apply this approach to prestressed membrane formworks it is necessary to extend to surface elements and combine with typical methods for flattening and stress compensation of cutting patterns in tensioned membrane structures.

3. Methodology

As an example and case study, the procedure outlined in this section is applied to one of four roof surfaces of PAB. The starting input provided by SO-IL and SBP are meshes representing the anticlastic exterior roof surfaces and a typical buildup of the roof (see Figure 2).

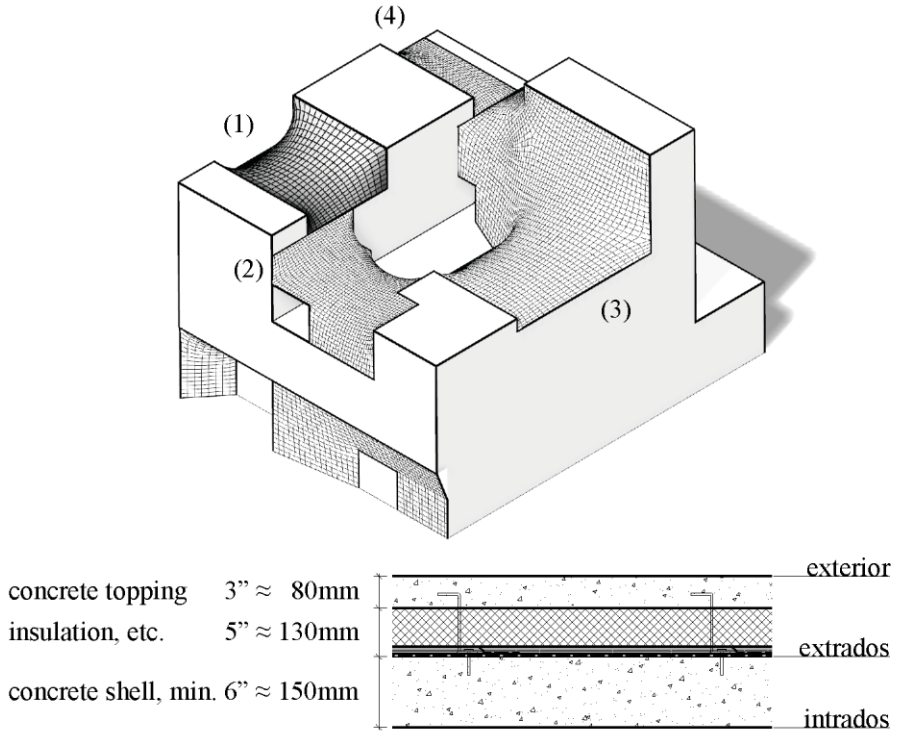

Figure 2: Four roof surfaces and typical section, where surface (1) is the example in the present paper

Figure 3 shows the different steps of the procedure to determine membrane stresses and reaction forces in the final, loaded state, and cutting patterns in the initial state. Starting from an input design shape, the key steps are to

1. pattern and mesh the target formwork surface;
2. determine target loads in final state; and
3. execute best-fit optimization to determine stresses in final state.

Then, if the deviations between target and best-fit shape exceed some threshold, update target shape and repeat steps 1-3. Otherwise,

4. flatten cutting patterns and map weave directions back onto target surface; and
5. materialize and compensate initial cutting patterns.

The resulting output can be used for further static analysis if necessary (e.g. live loads and/or sequencing).

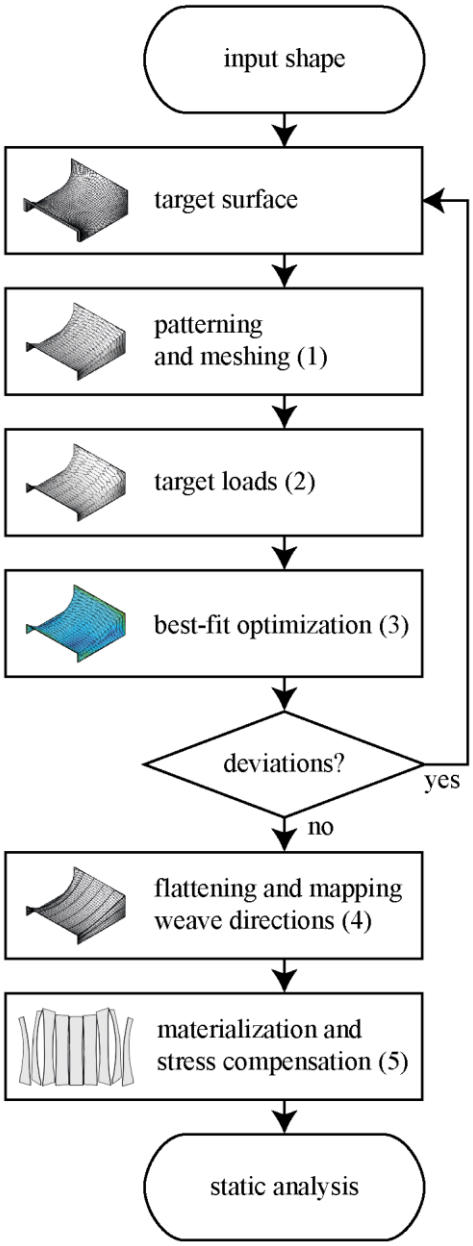

Figure 3: Flowchart of design process

3.1. Target formwork surface

The meshes that were provided as input shapes, represent the outer surface of the roof. For the formwork surface we require the interior i.e. intrados. Hence, the target mesh is offset by 360mm, the thickness of the entire roof buildup. A direct offset of this anticlastic mesh along the vertex normals creates two potential issues: the boundaries will no longer be straight, and the resulting mesh can intersect with itself. To avoid the former, the interior vertices are offset along their normal, but the

exterior vertices move only perpendicular to boundary planes. Then to avoid intersections, the offset is done iteratively in small increments, where at each step a Laplacian smoothing is applied.

3.2 Patterning and meshing

The resulting formwork mesh is divided along seam lines. Ideally, the seam lines coincide with the principal curvatures to reduce distortions of the cutting patterns (Seidel [14]) and follow geodesic lines along those directions to reduce cutting losses during fabrication (Moncrieff and Topping [6]). As a guideline, the principal curvatures are plotted (Figure 4a), and the 'hanging' direction is chosen as the general direction of the seams. In this case, additional constraints are that seams terminate at the edges, and do not meet in space, that they meet at corners of the boundaries, and that the distance between seams does not exceed the roll width, here assumed to be 2 m. This is done by manually selecting opposite boundaries for the patterns, which are then both automatically subdivided at points coinciding with corners on either side, and then subdivided further if their length exceeds 2 m (Figure 4b).

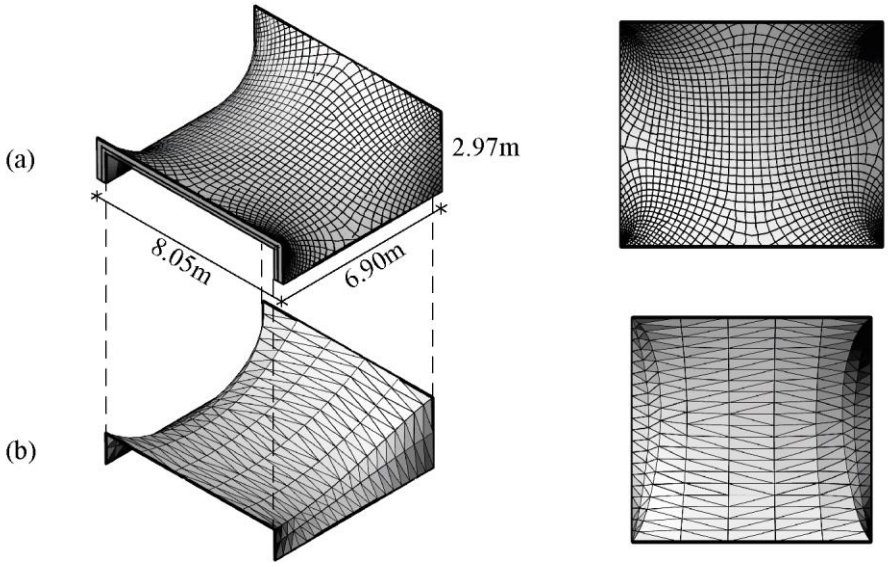

Figure 4: (a) Principal curvatures and (b) triangulated mesh following geodesic seam lines

3.3. Target load determination

The thickness of the shell varies between 150-250mm. At this stage, the exact geometry is not known, so a thickness of 150mm is assumed representative for most of the shell's surface. Assuming that the first concrete layer is cast entirely at once, we require the upper surface of the lower shell i.e. the extrados to determine the loads using the same offsetting process as in Section 3.1. The determination of membrane stresses is based on triangular elements (Figure 4b), so the surface, divided along the seam lines, is further discretized into a triangular mesh. The load for each vertex is calculated from the volume between its corresponding face in the dual diagram, and its projection on the extrados (Figure 5), multiplied by a concrete density of 25 kN/m^3. As such, the load is treated as self-weight rather than hydrostatic formwork pressure, assuming the mortar would be relatively viscous.

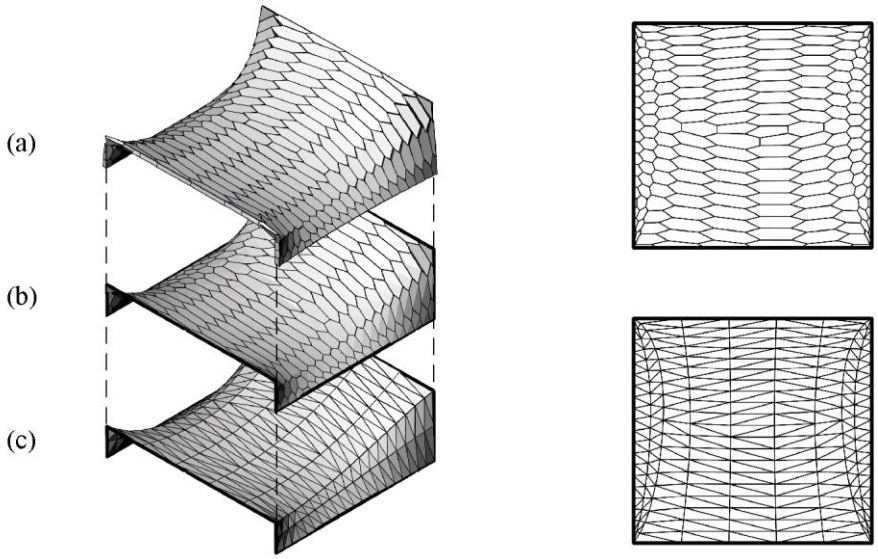

Figure 5: (a) Volumes of concrete load of vertices, (b) dual diagram of (c) original mesh.

3.4 Best-fit optimization

The goal is to find the force densities **q**, forces **f** or stresses **σ** such that, under given loads of the wet concrete, the resulting concrete shell takes the form of the target shape. The approach for discrete networks by Van Mele & Block [16] is extended to surfaces.

A branch-node matrix can be used to describe the topology of a network in form finding (Schek [13]). For a network with *m* branches and *n* nodes, the branch-node matrix is of size [*m* × *n*]. For networks consisting of *f* triangle elements Gründig [3] employed three separate [*f* × *n*] branch-node matrices, for each of the triangle sides. We assemble these in a single [3*f* × *n*] branch-node matrix **C**, so that the coordinate differences for all 3*f* element edges are $\mathbf{u} = \mathbf{Cx}$, $\mathbf{v} = \mathbf{Cy}$, $\mathbf{w} = \mathbf{Cz}$ where **x**, **y** and **z** are vectors of vertex coordinates.

The branch-node matrix and the coordinate vectors are split in two based on the $n = n_N + n_F$ free and fixed nodes $\mathbf{C} = [\mathbf{C}_N \quad \mathbf{C}_F]$, $\mathbf{x} = [\mathbf{x}_N \quad \mathbf{x}_F]$, $\mathbf{y} = [\mathbf{y}_N \quad \mathbf{y}_F]$ and $\mathbf{z} = [\mathbf{z}_N \quad \mathbf{z}_F]$.

We can define static equilibrium in each direction as

$$\begin{aligned} \mathbf{C}_N^T\mathbf{U}\mathbf{L}^{-1}\mathbf{f} &= \mathbf{C}_N^T\mathbf{U}\mathbf{q} = \mathbf{p}_x \\ \mathbf{C}_N^T\mathbf{V}\mathbf{L}^{-1}\mathbf{f} &= \mathbf{C}_N^T\mathbf{V}\mathbf{q} = \mathbf{p}_y \\ \mathbf{C}_N^T\mathbf{W}\mathbf{L}^{-1}\mathbf{f} &= \mathbf{C}_N^T\mathbf{W}\mathbf{q} = \mathbf{p}_z \end{aligned} \qquad (1)$$

where matrices **U**, **V** and **W** are the diagonal matrices of vectors **u**,**v** and **w**, **L** is a diagonal matrix of edge lengths and load vectors $\mathbf{p}_i$ are n_N loads acting in direction *i*. The resulting system of equations with *m* unknowns **q** or **f** and $3n_N$ equations is overdetermined:

$$\mathbf{Bq} = \mathbf{p} \text{ or } \mathbf{B}_f\mathbf{f} = \mathbf{p} \qquad (2)$$

where $\mathbf{B} = \begin{bmatrix} \mathbf{C}_N^T\mathbf{U} \\ \mathbf{C}_N^T\mathbf{V} \\ \mathbf{C}_N^T\mathbf{W} \end{bmatrix}$ or $\mathbf{B}_f = \begin{bmatrix} \mathbf{C}_N^T\mathbf{U}\mathbf{L}^{-1} \\ \mathbf{C}_N^T\mathbf{V}\mathbf{L}^{-1} \\ \mathbf{C}_N^T\mathbf{W}\mathbf{L}^{-1} \end{bmatrix}$, $\mathbf{p} = \begin{bmatrix} \mathbf{p}_x \\ \mathbf{p}_y \\ \mathbf{p}_z \end{bmatrix}$.

If we wish to enforce bounds on the force densities or forces (to avoid compressive stresses and stay within material tensile strengths), the resulting constrained linear least squares problem can be written as a quadratic program and solved as such (see Section 3.7). For example, in the case of bounded force densities:

$$\begin{aligned} &\min. \frac{1}{2}\mathbf{q}^T\mathbf{B}^T\mathbf{B}\mathbf{q} - \mathbf{p}^T\mathbf{B}\mathbf{q} \\ &\text{s.t. } \text{lb} \le \mathbf{q} \le \text{ub} \end{aligned} \tag{3}$$

Assuming the bounds have not allowed us to find an exact match with the target shape, we compute the coordinates of the best-fit result as in Schek [13]:

$$\begin{aligned} \mathbf{x}_N &= \mathbf{D}_N^{-1}\left(\mathbf{p}_x - \mathbf{D}_F\mathbf{x}_F\right) \\ \mathbf{y}_N &= \mathbf{D}_N^{-1}\left(\mathbf{p}_y - \mathbf{D}_F\mathbf{y}_F\right) \\ \mathbf{z}_N &= \mathbf{D}_N^{-1}\left(\mathbf{p}_z - \mathbf{D}_F\mathbf{z}_F\right) \end{aligned} \tag{4}$$

where $\mathbf{D}_N = \mathbf{C}_N^T\mathbf{Q}\mathbf{C}_N$, $\mathbf{D}_F = \mathbf{C}_N^T\mathbf{Q}\mathbf{C}_F$ in which **Q** is the diagonal matrix of vector **q**.

Applied to our case study, bounds are set on forces to keep them between 0.1 and 40 kN. Three iterations are required to update the target shape and have the resulting best-fit mesh be within 1mm deviation. This means the original design input has been altered to accommodate the fabrication method, with changes not exceeding 30mm (see Figure 6a).

3.5. Flattening patterns and mapping weave directions

To compute stresses it is necessary to determine the local (u,v) directions (see Equation (5)), chosen to coincide with the warp and weft directions to compare against material strengths later on. The mesh is first unrolled geometrically and an orthogonal (u,v) grid is generated on top of it (see Figure 7b). These directions are mapped back to the three-dimensional surfaces (Figure 7a) to determine local warp and weft directions for each triangular element.

The 3*f* force densities resulting from Equation (3) can then be converted to 3*f* stresses (Singer [15], Pauletti and Pimenta [9]). For a single element, the stresses are

$$\boldsymbol{\sigma} = \frac{1}{A}\mathbf{H}^T\mathbf{q}, \text{ since } \mathbf{q} = A\mathbf{H}^{-T}\boldsymbol{\sigma}, \tag{5}$$

where A is the triangle area,

$$\mathbf{H}=\begin{bmatrix} u_1^2 & v_1^2 & u_1v_1 \\ u_2^2 & v_2^2 & u_2v_2 \\ u_3^2 & v_3^2 & u_3v_3 \end{bmatrix}, \mathbf{H}^{-\mathrm{T}}=\frac{1}{4A^2}\begin{bmatrix} -v_2v_3 & -u_2u_3 & v_2u_3+u_2v_3 \\ -v_3v_1 & -u_3u_1 & v_3u_1+u_3v_1 \\ -v_1v_2 & -u_1u_2 & v_1u_2+u_3v_1 \end{bmatrix}, \boldsymbol{\sigma}=\begin{bmatrix} \sigma_{\mathrm{xx}} \\ \sigma_{\mathrm{yy}} \\ \sigma_{\mathrm{xy}} \end{bmatrix},$$

and *u* and *v* are local coordinate differences of triangle sides 1, 2 and 3 for each element. Combining Equations (2) and (5) we could also enforce bounds on the stresses,

$$\mathbf{BAH}^{-\mathrm{T}}\boldsymbol{\sigma}=\mathbf{p} \tag{6}$$

and in this case, the resulting solution would be dependent on the orientation of the elements.

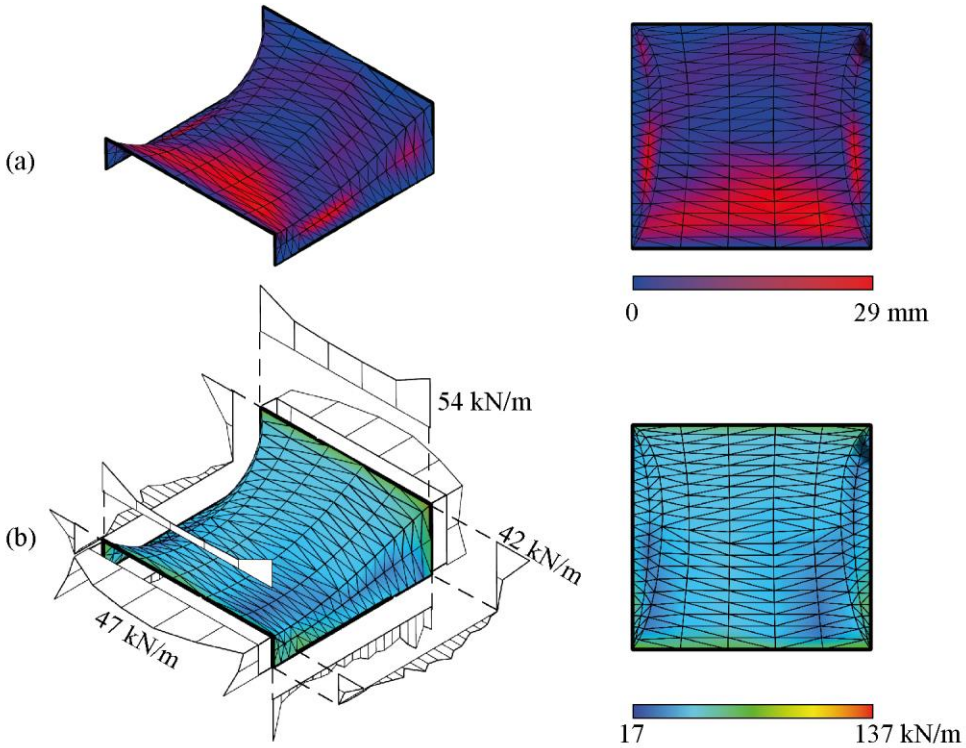

Figure 6: (a) Deviations between updated target mesh and original design input, (b) resulting Von Mises stresses and reaction stresses along the boundaries in (x,y,z) directions.

The resulting Von Mises stresses range between 17 and 137 kN/m under load of the full 150 mm of fresh concrete. The upper limit is in the order of strengths corresponding to type IV to V PVC-coated polyester fabrics. This stress occurs locally, and the fabric could potentially be multiplied here to meet

required safety factors. Note that our load case is of a temporary nature until the concrete has sufficiently cured.

3.6. Materialization and stress compensation

By choosing a material model and properties, we can calculate the initial geometry of our cutting patterns, allowing us to compensate for the prestress. In our case, we assume an isotropic material model with Young's modulus of E = 1500 kN/m and Poisson's ratio of ν = 0.2, so the constitutive equation is

$$\boldsymbol{\sigma} = \mathbf{D}\boldsymbol{\varepsilon} \tag{7}$$

where $\mathbf{D} = \frac{E}{1-\nu^2}\begin{bmatrix} 1 & \nu & 0 \\ \nu & 1 & 0 \\ 0 & 0 & (1-\nu)/2 \end{bmatrix}$

The strain can be expressed as (Singer [11], Pauletti and Pimenta [6]):

$$\boldsymbol{\varepsilon} = \frac{1}{2}\mathbf{H}^{-1}\left(\mathbf{L}\mathbf{l} - \mathbf{L}_0\mathbf{l}_0\right) \tag{8}$$

where subscript 0 refers to the initial, slack edge lengths of the triangle. By combining Equations (5), (7), and (8), we can write the squared initial lengths as a function of the known force densities

$$\mathbf{L}_0\mathbf{l}_0 = \mathbf{L}\mathbf{l} - \frac{2}{A}\mathbf{H}\mathbf{D}^{-1}\mathbf{H}^{\mathrm{T}}\mathbf{q} \tag{9}$$

and by taking the square root, we have found the initial lengths, which allow us to calculate the compensated cutting patterns (Figure 7c).

3.7. Implementation

The entire design process was implemented in Grasshopper for Rhinoceros (Rutten [12], McNeel [7]). Several plug-ins for Grasshopper were included: Millipede to plot principal curvatures, Hoopsnake for iterative processes within the definition, and various mesh operations possible with BullAnt, Kangaroo, Lunchbox, MeshEdit, Starling and Weaverbird (McNeel [8], Rutten [12]). A number of custom C# and IronPython components were written: to generate geodesic lines on a mesh; to subdivide and convert the mesh to surfaces and flatten them; and, to communicate with an external CPython script for the best-fit optimization, which uses CVXOPT's QP solver (Andersen *et al.* [1]) to solve the bounded least-squares problem.

4. Discussion

Noticing that the outer patterns have become quite distorted (Figure 7c), we need to remap the (u,v) directions and iterate again. This is uncommon in patterning for tensioned membrane structures,

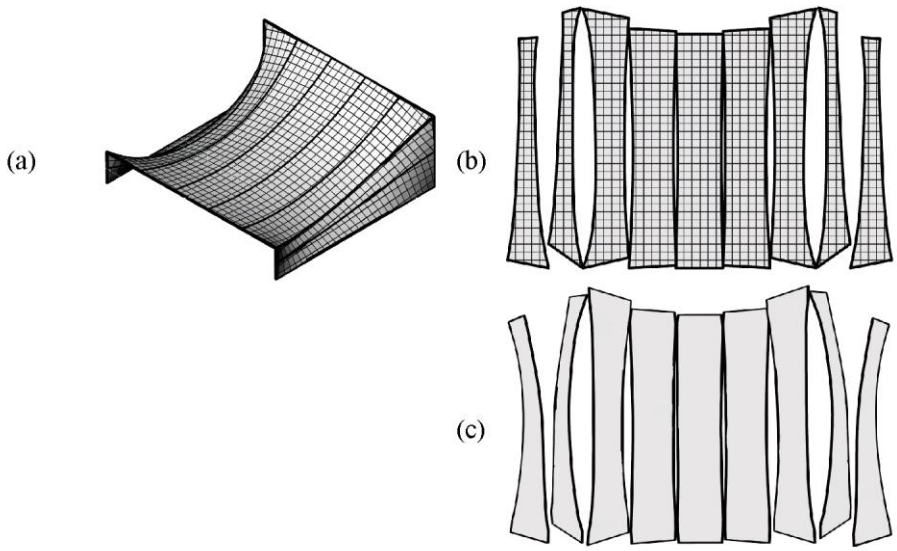

Figure 7: (a) Warp and weft (u,v) directions mapped onto the surface, from (b) the flattened cutting patterns, and (c) after stress compensation.

which are generally designed to have either uniform stress (e.g. saddle shape roofs) or symmetric patterns along gradients of stress (e.g. high point roofs), both of which would result in symmetric stress compensation. In our case, it is a logical outcome given that we design for a loaded rather than evenly or smoothly stressed membrane. It would be interesting to optimize the seam lines in such a manner that the distortions would no longer lead to higher cutting losses.

The design process can be further improved by looping the distorted cutting patterns (Figure 7c) back into the stress calculation or even to the very beginning if limits on the stresses (or strains) are included. This could be relevant if additional constraints on the patterns are directly included, such as minimizing strains along the boundary (to avoid having to prestress parallel to the boundary), or enforcing equal strains between adjacent seams to avoid potential wrinkling along seam lines.

The results of our design process will be validated through the construction and measurement of a 1:4 prototype, and the comparison of the geometry and stresses with those resulting from the computational model. The measurements will have the same objectives as that of previous work on a cable-net formed prototype (Veenendaal et al. [13]), but use methods more appropriate to measuring stresses and strains in fabrics.

5. Conclusions

This paper presented a computational design workflow for a prestressed membrane formwork of a given anticlastic shell structure. It intended to reduce construction tolerances through the precise determination of membrane stresses and corresponding cutting patterns. To this end, this workflow combined best-fit optimization for discrete networks with triangular elements, flattened strips of those elements, and subsequently compensated them for stress.

Acknowledgements

The authors would like to thank Florian Idenburg from SO-IL for inviting us to investigate the use of fabric formworks in PAB and using it as a case study for our research, as well as Kevin

Lamyuktseung from SO-IL for providing information on the project, and discussing its design and construction.

References

[1] Andersen, M.S., Dahl, J. and Vandenberghe, L., CVXOPT, http://cvxopt.org, 2014

[2] Cauberg N., Parmentier B., Vanneste M. and Mollaert M. Fabric formwork for flexible, architectural concrete, in *Proceedings of the International Symposium on Fibre-reinforced Polymer Reinforcement for Concrete Structures, FRPRCS-9*, Oehlers D., Griffith M. and Seracino R. (eds.), Sydney; 2009.

[3] Gründig L., Minimal surfaces for finding forms of structural membranes. *Computers & Structures*, 1988; **30**; 679-683.

[4] Kersavage J.A., Method for constructing a tensile-stress structure and resultant structures. US Patent 3,927,496; 1975.

[5] Knott A. and Nez G., *Latex Concrete Habitat*. Trafford Publishing Company; 2005

[6] Moncrieff E. and Topping B.H.V., Computer Methods for the Generation of Membrane Cutting Patterns, in *Computers & Structures*, 1190; **37**(4); 441-450.

[7] McNeel, R., Rhinoceros, http://www.rhino3d.com, Robert McNeel & Associates, 2014

[8] McNeel, R., Food4Rhino, http://www.food4rhino.com, Robert McNeel & Associates, 2015

[9] Pauletti R.M.O. and Pimenta P.M., The natural force density method for the shape finding of taut structures, *Computer Methods in Applied Mechanics and Engineering*, 2008; **197**; 4419-4428

[10] Pedreschi R. and Lee D.S.H., Structure, form and construction. Fabric formwork for concrete, in *Across: Architectural Research through to Practice: 48th International Conference of the Architectural Science Association 2014*, Madeo F. and Novi F. (eds.), The Architectural Science Assocation, 2014, 99-110.

[11] Pronk A., Houtman R. and Afink M., The reconstruction of the Philips pavilion, Volume 1, in *Sources of Architectural Form, Theory and Practice*, Kuwait City; 2007.

[12] Rutten, D., Grasshopper, http://www.grasshopper3d.com, 2015

[13] Schek H.-J., The force density method for form finding and computation of general networks. *Computer Methods in Applied Mechanics and Engineering*, 1974; **3**; 115-134.

[14] Seidel M., Tensile Surface Structures. A Practical Guide to Cable and Membrane Construction, Ernst & Sohn, 2009.

[15] Singer P., Die Berechnung von Minimalflächen, Seifenblasen, Membrane und Pneus aus geodätischer Sicht, Ph.D. thesis, University of Stuttgart, Germany, 1995.

[16] Van Mele T. and Block P., Novel form finding method for fabric formwork for concrete shells. *Journal of the International Association of Shells and Spatial Structures* 2011; **52**(4):217–24

[17] Veenendaal D., West M. and Block P., History and overview of fabric formwork: using fabrics for concrete casting. *Structural Concrete - Journal of the fib*, 2011; **12**; 164-177.

[18] Veenendaal D. and Block P., Design process for prototype concrete shells using a hybrid cable-net and fabric formwork. *Engineering Structures* 2014; **75**:39-50.

[19] Veenendaal D., Bezbradica M., Novak D. and Block P., Controlling the geometry and forces of hybrid cable-net and fabric formworks. *Proceedings of the IASS-SLTE 2014 Symposium*, Brasilia; 2014.

[20] Waller J.H.d.W. and Aston A.C., Corrugated concrete shell roofs. *Proceedings of the Institution of Civil Engineers*, 1953; **2**(4); 153-182.

[21] West M. and Araya R., Fabric formwork for concrete structures and architecture, in *Proceedings of the International Conference on Textile Composites and Inflatable Structures, Structural Membranes 2009*, Krõplin B. and Oñate E. (eds.), Barcelona; 2009.